DEVELOPMENT OF CATHODE CONTACTING FOR SOFC STACKS

K. Sick, N. Grigorev, N.H. Menzler, and O. Guillon Forschungszentrum Jülich, Institute of Energy and Climate Research, Materials Synthesis and Processing (IEK-1), Jülich, Germany

ABSTRACT

In SOFC stacks the electrical contact between the ceramic cathode layer and the metallic interconnector (IC) has to be adjusted carefully to minimize the contact resistance and slow down degradation mechanisms. In JÜLICH, ICs made of Crofer22APU are coated with a $MnCo_{1.9}Fe_{0.1}O_4$ spinel (MCF), applied by atmospheric plasma spraying (APS), which successfully prevents the diffusion of volatile Cr species from the steel into the cell. Materials for the cathode contact layer have to be sufficiently good electronic conductors, stable in oxidizing atmosphere, chemically stable and compatible with the adjacent layers, and show a thermal expansion behavior similar to MCF and the cathode material, i. e. $La_{0.58}Sr_{0.4}Co_{0.2}Fe_{0.8}O_{3-x}$ (LSCF).

To obtain an optimal contact layer, different aspects such as material properties, microstructure, and processing have to be considered. Here we compare various materials regarding their electrical conductivity and compatibility with each other and discuss different processing routes for the application of the cathode contact layer. DC conductivity measurements and scanning electron microscopy (SEM) imaging give information on the correlation of material properties and microstructure. We conclude that an LSCF contact layer with coarse porosity on top of the fine structured LSCF cathode is the most suitable contacting for JÜLICH SOC stacks.

INTRODUCTION

Fuel cells are always being optimized for more power output, making the various layers thinner for less ohmic resistance and adjusting the interfaces for less polarization resistance. But when several cells are put together into a stack not only the cell values but also the interconnecting elements become important and a good contact from the cells to the connecting elements is required.^{1, 2}

Interconnectors (IC) establish the electrical connection between the individual stack planes and the gas distribution across the cells. In JÜLICH, a Ni mesh is used as contacting layer between the anode substrate and the IC at the fuel side, and a contact layer either printed onto the cathode or applied to the IC is used at the cathode side.^{3, 4} This contact layer has to be a good electrical conductor, be stable at high temperature under oxidizing atmosphere, be chemically compatible with the adjacent materials, and have a thermal expansion coefficient (TEC) similar to the coefficients of the materials in neighboring components.⁵ These features will be discussed here.

For reasons of easy fabrication and good electrical conductivity, Cr-based ferritic steels such as Crofer22APU are commonly used for interconnecting elements.^{6, 7} The naturally formed chromia scale protects the material from excessive corrosion and oxidation at high temperatures and has an acceptable electrical conductivity compared to silica or alumina whose amounts are kept to a minimum level in Crofer22APU.^{8, 9, 10} The disadvantage of the Cr-based steel is the release of volatile Cr species at SOC operating temperatures, especially in the presence of water vapor, which cannot be excluded when operating a stack under realistic conditions.^{11, 12} The volatilized Cr adsorbs onto the cathode or contact layer surface and causes degradation. This poisoning of the cathode side happens via the formation of detrimental SrCrO₄ crystallites with a low electrical conductivity, which block the pores and hence the gas supply of the cathode.^{13, 14, 15, 16} To prevent the poisoning, the Crofer22APU is coated with a protective layer that either is dense enough to hinder Cr diffusion via the gas phase or acts as a Cr getter, for instance by offering a reaction partner that holds the evaporated Cr in a layer near to the Crofer22APU surface.¹⁷ In JÜLICH, this protective

coating is made of MnCo_{1.9}Fe_{0.1}O₄ (MCF) and applied by atmospheric plasma spraying (APS) onto the ICs. ^{18, 19} This coating is dense and has proven its ability for the retention of Cr. ^{4, 13, 14, 15, 20} The electrical conductivity of MCF at 800°C amounts to 26-30S/cm²¹ and the TEC is about 13·10⁻⁶/K (30-800°C)^{21, 22} which is comparable to the TEC of Crofer22APU with 11.9·10⁻⁶/K (30-800°C)¹⁰. Other types of coating materials are manganese oxide or manganese cobalt oxides and numerous application techniques yielding more or less dense coatings are reported in literature. ^{16, 21, 23, 24, 25, 26, 27, 28, 29, 30, 31, 32, 33, 34, 35, 36} Concerning JÜLICH stacks, highest power output is reached with an APS MCF protective coating compared to a wet powder sprayed (WPS) MnOx coating. ^{4, 15, 21}

Thus, one interface of the contact layer is towards the protective coating. The second interface is the one towards the cathode, which in JÜLICH consists of LSCF (La_{0.58}Sr_{0.4}Co_{0.2}Fe_{0.8}O₃). LSCF has a remarkably higher TEC than the formerly used LSM (Sr-doped La-Mn perovskite) as a compound with YSZ for improved ionic conductivity in the cathode – approx. $15 \cdot 10^{-6} / K^{37, 38}$ compared to approx. $12 \cdot 10^{-6} / K$ (both 30-800°C)^{27, 38}. But LSCF is a MIEC material itself and yields a higher power density. As a disadvantage, LSCF is more prone to poisoning by impurities (sulfur, silicon) and to Sr segregation at the surface in combination with the formation of undesired phases than LSM. ^{39, 40, 41, 42} But as the power is higher and degradation could be slowed down by protective coatings, LSCF is the material of choice. Especially when the operation temperature is lowered to 600-800°C, the electrical conductivity of LSCF is much higher than of LSM. ⁴³ Alternatively, LSC, a Sr-doped La-Co perovskite, could be used as cathode material. LSC has an even higher conductivity for electrons than LSCF but the TEC is also higher, which might cause problems during thermal cycling of such a cell, and the ionic conductivity is lower than for LSCF. ^{5, 38}

Considering the protection layer and the cathode material, the contact layer should have a TEC of 13-19·10⁻⁶/K and a good electrical conductivity. An overview of possible materials for the cathode contact layer can be found in literature. ^{3, 44, 45} In JÜLICH, a Co- and Cu- doped La-Mn perovskite composition called LCC10 has been the standard for some years. ^{4, 5, 46, 47, 48} Recently, LSCF has also been tested as a contact layer material with perfect compatibility to the LSCF cathode. Alternatively, Sr- and Co-doped La-Mn perovskite (LSMC) or even LSC might be used. Here we compare LCC10, LSCF, LSMC, and LSC with regard to the suitability, intrinsic material properties, microstructural effects, and influences due to processing. In Table I the relevant materials and their properties are listed. The aim is to minimize the contact resistance between interconnector and cathode while keeping the production easy and cheap by an optimal selection of material, microstructure, and processing. ⁴⁸

Table I. Properties of some SOC materials

Layer	Name	σ _{e-} / Scm ⁻¹ at 800°C	TEC / 10 ⁻⁶ K ⁻¹ for 30-800°C
Interconnector	Crofer22APU	8700 10	11.9 10
Protective coating	MCF	26-30 ²¹	~13 ^{21, 22}
Protective coating	MnOx	0.1 49	8.8 49
Contact layer	LSMC	~180 38	12-16 ^{27, 38} (30-1000°C)
Contact layer	LCC10	~80 46	~14 46
Contact layer,	LSCF	100-200 37, 38	13-16 ^{37, 38} (30-1000°C)
Cathode			
Cathode	LSC	>1220 38	19 ³⁸ (30-1000°C)
Cathode	LSM	~160 38	11-12.4 ^{27, 38} (30-1000°C)

EXPERIMENTAL

Electrical conductivity measurements

The electronic conductivities of LSCF, LCC10, LSMC, and LSC are measured on pressed and pre-sintered pellets. The pellets are contacted by two platinum meshes pressed onto the sample during the measurement. The samples are heated up to 850° C and kept at this temperature for several hours before cooling down with 5K/min. Meanwhile a constant current of 1A (corresponding to approx. $0.5A/cm^2$) is applied to the sample and the voltage is measured by a multimeter with a resolution of $10\mu V$. These measurements yield the conductivity of porous samples. By taking the dimensions (size and weight) of the pellets, measuring the density by the Archimedes method, and estimating the porosity from microscopy images via setting a threshold, the relative densities of the pellets are obtained by comparison to the theoretical densities.

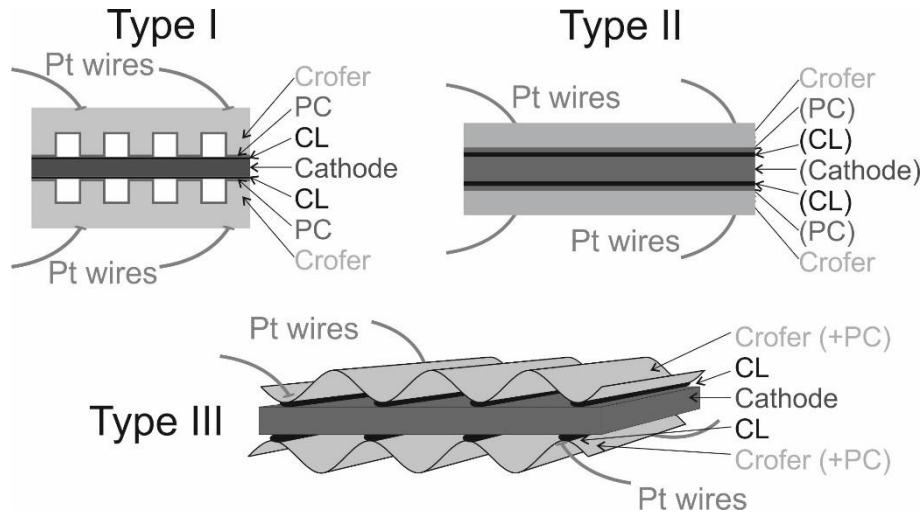


Figure 1. Three sample geometries are used. All samples have a symmetric setup with metallic interconnector elements at the top and at the bottom for easy and reproducible contacting via platinum wires. The cathode in the sample center consists of a pressed and sintered LSCF pellet.

Contact resistance measurements

For stack operation not only the intrinsic material features but especially the properties of the layered system with several interfaces are important. In order to measure a simple but roughly realistic sample system we build symmetric samples according to Figure 1. The systems comprise IC parts (with a channel-rib-structure) at the top and at the bottom, including the protective coating (PC) (if applied to a certain sample) on the corresponding inside of the element. The contact layer (CL) is printed onto the full area of the cathode (both sides) for sample Type I, onto the pre-coated IC elements for sample Type II, and onto the interconnector ribs as stripes of 1.5mm width for sample Type III. An LSCF pellet (pressed and sintered) polished to approx. 14mm by 14mm is used as the cathode in the center of the sample sandwiches.

For contacting the samples, platinum wires are spot welded by laser welding to the IC pieces. Each sample has four wires, two at the top and two and the bottom, for separate U-and I-connections. A current of 1A is lead diagonally through the sample, corresponding to a current density of $0.5 \, \text{A/cm}^2$ which is a frequently used value in stack tests⁵⁰. The voltage drop across the sample is measured via the other two wires. For contact resistance measurements the samples are heated up to $850 \, ^{\circ}\text{C}$, which is the stack sealing temperature for JÜLICH stacks, and kept there for 10h. At the moment, the sealing time at JÜLICH is 100h due to the glass sealings but a shorter sealing time of 10h is basically aimed at. Current and voltage

values are recorded during the cooling process of 5K/min. During the entire procedure, the samples are pressed together with a weight of approx. 500g/cm².

The contact resistance is usually plotted as area specific resistance (ASR) dependent on the temperature ("operation temperature"). The ASR as the product of total resistance R and active sample area A is a useful tool to compare the resistances of samples with different areas but a similar setup in their cross section perpendicular to the current flow. Hence, we can compare the ASR values measured on the mentioned symmetric samples to ASR values measured for a single (contacted) cell or a layer in a stack.

Microscopic investigations

To obtain an insight into the microstructure of surfaces and interfaces, scanning electron microscopy (SEM) is applied for imaging sample surfaces and cross sections. By this method, the porosity can be estimated from the images and subsequently the results can be correlated to conductivity and resistance measurements.

RESULTS AND DISCUSSION

Comparison of contact layer materials

Our measurements of the conductivities of porous samples, shown in Figure 2, are partly in agreement with literature yielding the highest conductivity for LSC⁴⁴. We observe the second highest value for LSCF while LSMC and LCC10 show values that are rather low compared to the other two materials. The deviations might be explicable considering the deviating microstructures of the pellets investigated here resulting from powders with very different particle size distributions and pre-treatments. The LSCF, LCC10, and LSC powders made in JÜLICH have a coarse structure with grains of 1-50 µm size and received a heat treatment of less than 1000°C. The LSMC powder provided by a project partner contains much finer particles of less than 1µm grain size with agglomerates of up to 100µm and has probably been annealed up to 1100°C. Hence, the sinterability of LSMC at 1200°C is much lower than for the other powders and the LSMC pellet remains more porous as proven by SEM graphs in Figure 3.

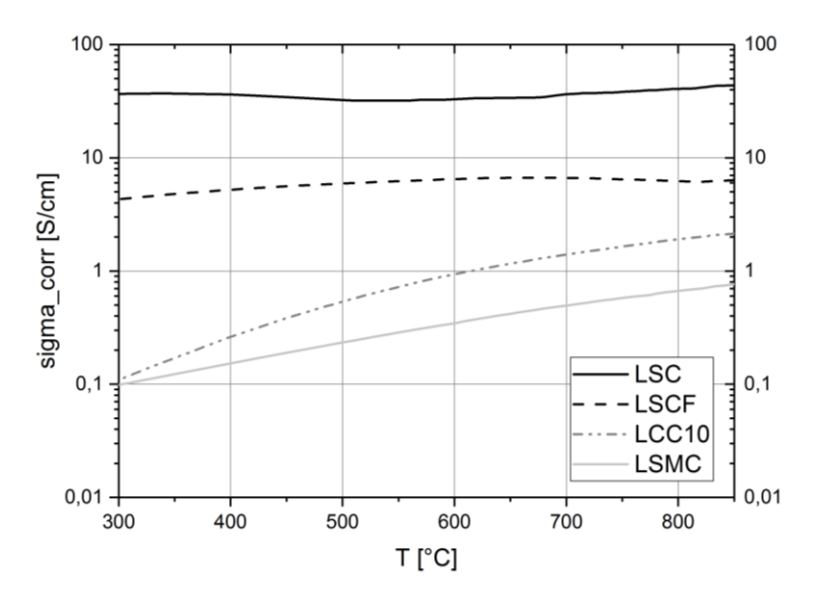


Figure 2. Electronic conductivities of four materials in dependence on temperature.

As the samples used here are not completely dense, we applied several methods to obtain values for the density of the samples and correlated the conductivity with the achieved density.^{47, 51} In the diagram in Figure 2 the conductivity values are shown with the sample porosity considered according to the formula suggested by Tietz et al.⁴⁷ Obviously the

conductivity values measured here are about one order of magnitude lower than reported in literature (c.f. Table I), which is most probably due to the not optimal contacting by pressing platinum meshes onto the samples. Nevertheless, LCC10, LSCF, and LSMC have been considered for the next experiments where they have been applied as a layer between an LSCF cathode and the protective coating on the interconnector. LSC was not considered further as a contact material since its high TEC is assumed to cause problems when the stack temperature is changed.

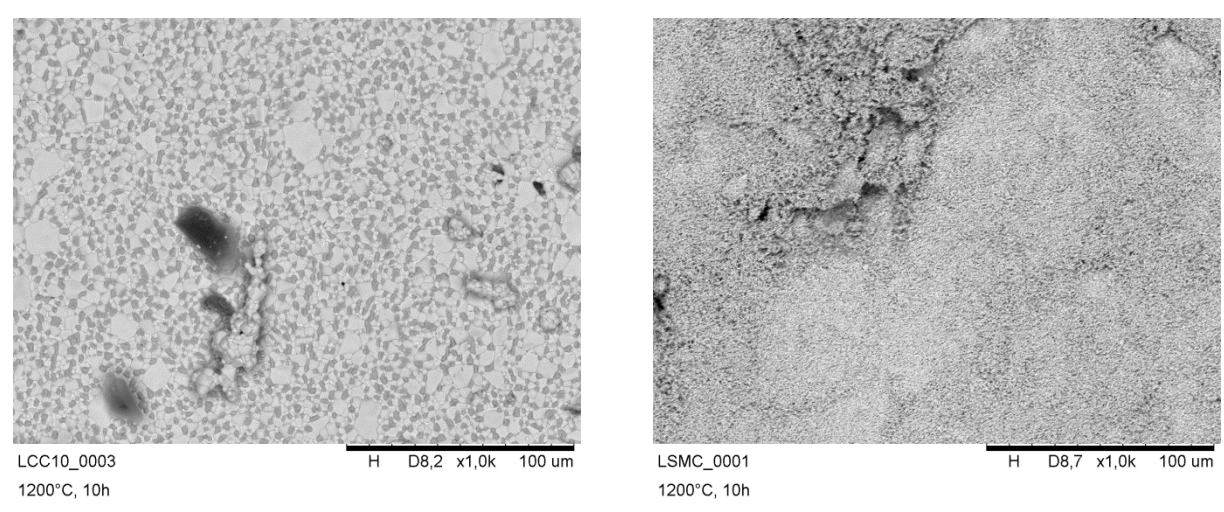


Figure 3. SEM surface images of pressed and sintered (1200°C) pellets used for conductivity measurements. Left: LCC10 with high sinterability and coarse particles. Right: LSMC with low sinterability and very fine particles.

Three samples are set up according to Figure 1, Type I, as symmetric sample sandwiches with the channel-rib structure typical for JÜLICH SOC stacks. The contact material is prepared as a paste and screen printed onto the entire surface on both sides of the cathode pellet. After drying, the sample is placed into a furnace and the contact resistance is measured as described above. Figure 4 depicts the ASR for the samples with different contact layer materials in dependence of the "operation" temperature after a sealing time of 10h at 1090°C. The lowest resistance is achieved with the sample that has an LSCF contact layer but the other two samples have an only slightly higher resistance. Here is becomes clear that not only the material's electronic conductivity determines the performance (el. cond. LSCF > LCC10 > LSMC), but the microstructure becomes important in thin and porous layers overruling the material properties partly (LCC10 is coarse with higher conductivity compared to LSMC which has less conductive but is fine-grained; but both show similar ASR results as porous layer).

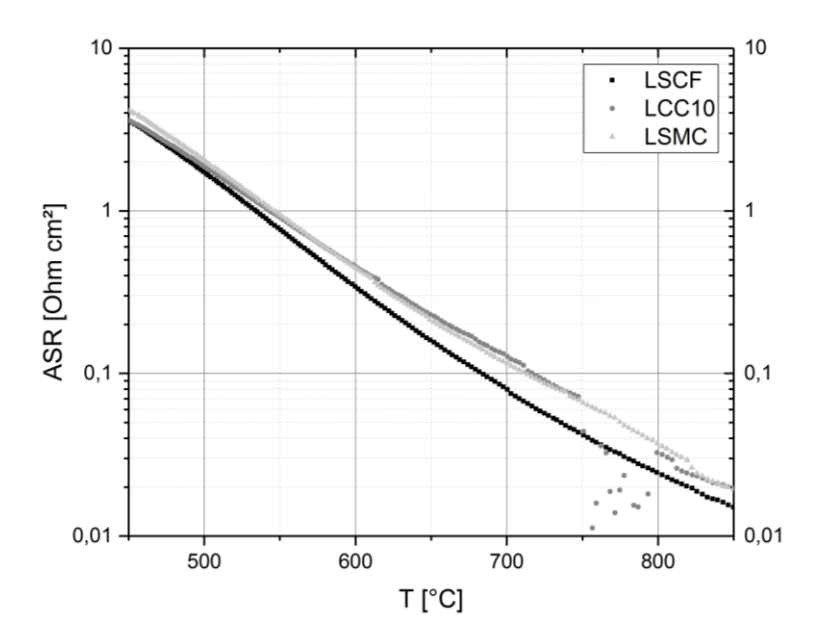


Figure 4. Contact resistances of samples with different contact layer materials in dependence on the operation temperature.

Contributions of layers and interfaces to the total contact resistance

In order to identify the layer(s) or interface(s) with a high or low contribution to the overall contact resistance, meaning the total resistance measured between IC and cathode, symmetric samples were set up with fewer layers, according to Type II and III in Figure 1. The resistances plotted in Figure 5 belong to the following layer combinations:

- "IC+PC_{APS}" means IC with protective coating applied by APS without contact layer and cathode in the sample center.
- "IC+PC_{APS}+CL_{LSCF}" means IC with protective coating (APS) with LSCF contact layer without cathode in the center.
- "full" means a full sample (IC, PC either by APS or WPS, contact layer and cathode).
- "IC+PC_{WPS}+cath" means IC with protective coating applied by WPS with cathode in the center but without contact layer.
- "IC+CL_{LSCF}+cath" means IC without protective coating but with LSCF contact layer and cathode.
- "IC_{ox}+CL_{LSCF}+cath" means IC without protective coating but pre-oxidized with LSCF contact layer and cathode.

Interestingly, the "full" samples (red, orange and green symbols) with three interfaces (IC-PC, PC-CL, and CL-cathode) have the second lowest resistance at 500-700°C. The lowest resistances for T>500°C (IC-PC_{APS}, red, and IC+PC_{APS}+CL_{LSCF}, orange) are achieved with samples comprising no cathode pellet. The reason for this fact could be that the relatively thick pellet used here contributes a non-negligible ohmic resistance. On the other hand, the total resistance of the full samples is still lower by a factor of 5-10 than the resistances of samples without a protective coating (IC_{ox}+CL_{LSCF}+cath, blue triangles), at least for T>500°C. This means that already in the beginning of stack operation (as simulated in our experiments) the protective coating is important for lowering the contact resistance. Later during long-term operation, the coating will result in a decreased degradation rate. The sample IC+PC_{WPS}+cath (green crosses) shows a similar resistance as the full samples with a contact layer at T>750°C. For lower temperature the resistance is slightly higher without the contact layer. Thus, from the presented measurements we conclude that the contact layer itself and its interfaces to the cathode and to the protective coating contribute a certain but not too large part to the total contact resistance of the sample. The most important layer to include is the protective coating

as it conveys the transition from the otherwise corroding metal to the porous, susceptible, easy poisonable ceramics. The role of the contact layer is to adjust the transition from the protective coating to the cathode, especially for T<750°C. In addition it is used to level height differences during the stack assembly and with its coarse porosity it assures a sufficient supply of air to the fine-structured cathode.

Performance of two contact layer materials in combination with different protective coatings

The previous investigations made us aware of the importance of the protective coating in combination with the contact layer. Now we measure contact resistances for seven different combinations of protective coating and contact layer material. All samples have the Type III geometry (Figure 1) and an LSCF cathode pellet in the center. The combinations are:

- IC_{ox}, LSCF: pre-oxidized IC metal but no protective coating, LSCF contact layer
- ICox, LSMC: pre-oxidized IC metal but no protective coating, LSMC contact layer
- WPS, LSCF: IC with MCF PC applied by WPS, LSCF contact layer
- WPS, LSMC: IC with MCF PC applied by WPS, LSMC contact layer
- WPS_red+ox, LSCF: IC with MCF PC applied by WPS and 2-step reactive sintering (for densification), LSCF contact layer
- APS, LSCF: IC with MCF PC applied by APS, LSCF contact layer
- APS, LSMC: IC with MCF PC applied by APS, LSMC contact layer

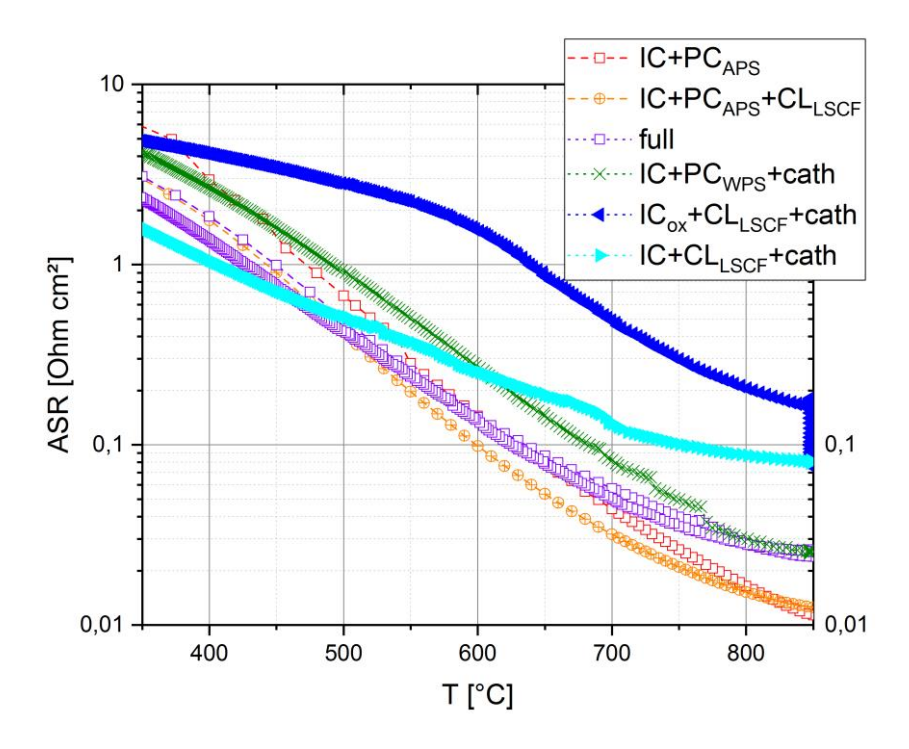


Figure 5. Contact resistances of samples with varying amounts of layers and interfaces in dependence on the operation temperature. For abbreviations see Figure 1 (in state "full" two samples have been characterized for reproducibility test).

We expect the samples with an APS PC to show the lowest and the samples without a PC the highest contact resistance. Usually, with a WPS PC the resistance is higher than with an APS coating due to the lower density and ability for chromium retention of the WPS coating, as mentioned above. Thus, APS has been applied for many years at JÜLICH although this method is rather complicated and time consuming. WPS is less complex but does not yield dense coatings unless combined with a heat treatment of the sprayed sample called reactive sintering. During two sintering steps, first in reducing atmosphere and subsequently in oxidizing atmosphere, the structure of the sprayed material changes in a way

that a final density is obtained that seems sufficient for chromium retention. Similar effects haven been reported for manganese-cobalt-oxides. 17, 28, 30, 36, 52, 53 In Figure 6 two electron microscopy images of cross sections are shown, one with the conventional APS protective coating and one with the newly developed coating applied by WPS and densified by reactive sintering.

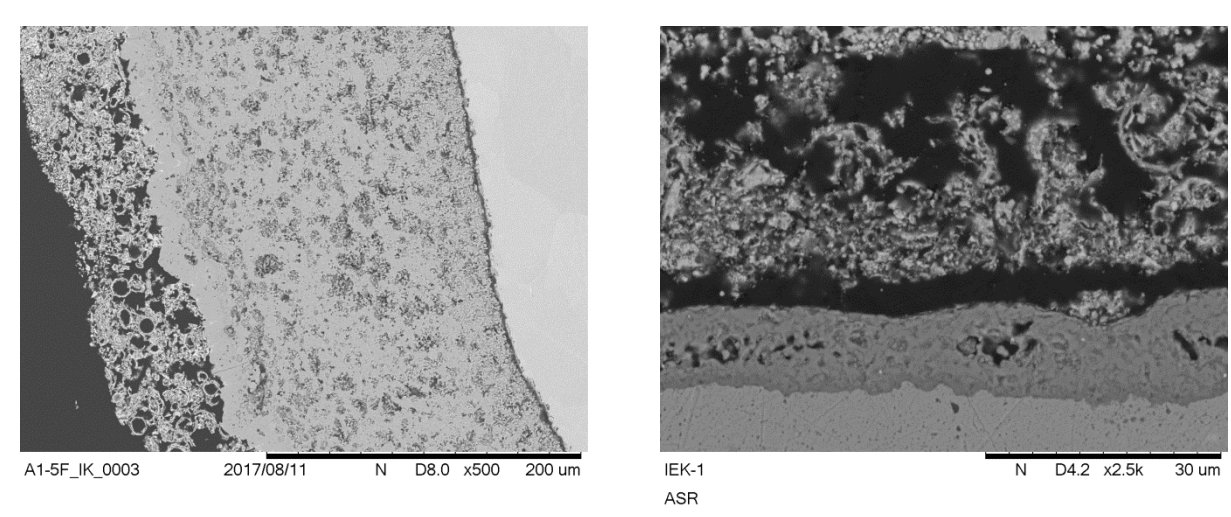


Figure 6. Cross sections in SEM. Left: MCF protective coating on Crofer 22 APU applied by APS and highly porous LSCF contact layer applied by screen printing. Right: MCF protective coating on Crofer 22 APU applied by WPS and reactive sintering for densification, LSCF contact layer.

Figure 7 depicts the contact resistances of the samples with different PC-CL combinations. The samples without any protective coating (ICox) have the highest and the samples with a PC applied by APS have the lowest electrical contact resistance, just as expected, at least for temperatures above 600°C. The samples with a PC applied by WPS have about twice the resistance than the samples with an APS PC. Interestingly, the two samples with an LSMC contact layer (dashed lines) and either an APS coating (light grey) below or without a protective coating (black) have a lower resistance than the corresponding samples with an LSCF contact layer (solid lines). For the APS samples, this is probably due to the finer microstructure of the LSMC layer due to smaller initial particle sizes. A finer network offers more paths for electrons to pass through the layer and hence the resistance is smaller. For the samples without a protective coating, there might occur an additional effect reducing the resistance: LSMC contains manganese which is a favored reaction partner of chromium to form a Cr-Mn spinel. Hence, the LSMC layer acts as a getter for the detrimental volatile Cr species and prevents them to poison the cathode, which would become visible in an increasing resistance. With a WPS protective coating, some of the Cr is blocked by this PC and both contact layers show a similar performance because LSCF has the higher conductivity but LSMC has the finer structure and in addition getters some diffusing Cr species. The coarse and highly porous microstructure of the LSCF contact layer is given in Figure 6 and the microstructures of an LSMC contact layer and a protective coating applied by WPS without a subsequent heat treatment are given in Figure 8.

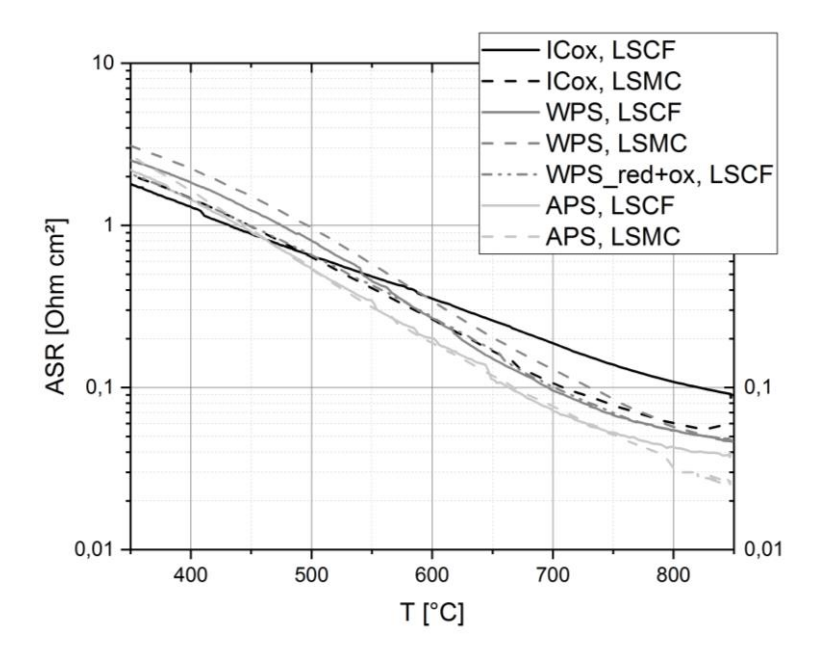


Figure 7. Contact resistances of samples with different combinations of protective coating and contact layer in dependence on the operation temperature.

From these measurements we conclude that the dense APS protective coating offers the best Cr retention and the lowest contact resistance. The alternative WPS coatings show a similar performance in the experiments conducted here. Nevertheless, for a conclusive study, long-term stack tests have to be evaluated regarding the degradation rates achieved with these layer combinations.

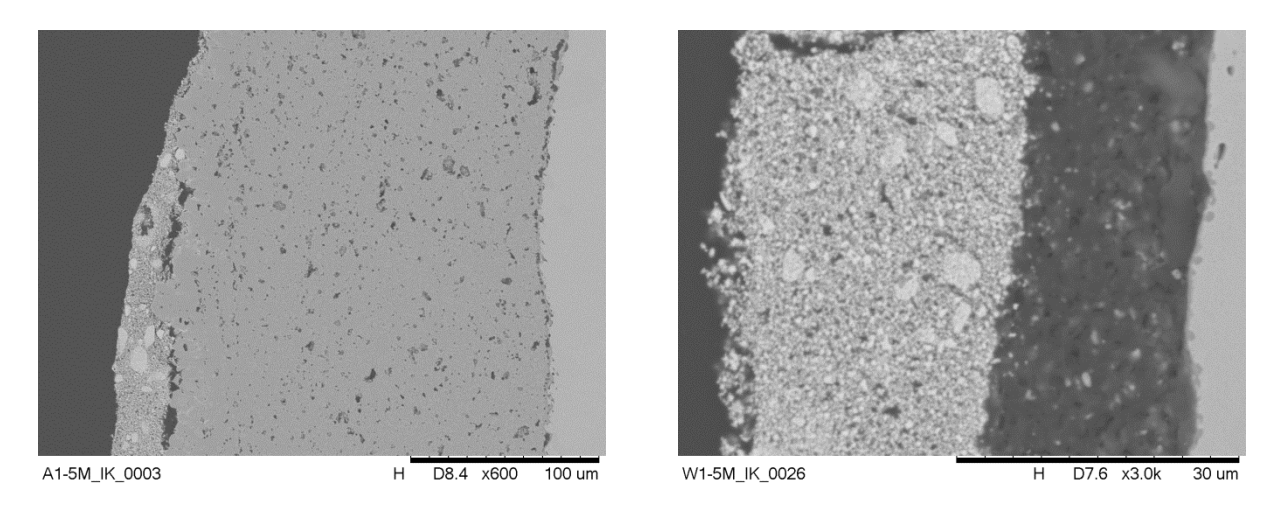


Figure 8. Cross section in SEM. Left: MCF protective coating on Crofer 22 APU applied by APS and rather dense and thin LSMC contact layer applied by screen printing. Right: MCF protective coating on Crofer 22 APU applied by WPS (no heat treatment) and fine structured LSMC contact layer.

Effect of the contact layer thickness

As mentioned before, one task of the contact layer is to level height differences in a stack, especially during assembly and sealing. We varied the contact layer thickness and conducted resistance measurements to observe the effect of the layer thickness. The sample geometry is Type III, the protective coating is the same for all six samples of which three have an LSMC and the other three an LSCF contact layer. To vary the thickness, the contact layer was screen printed up to three times onto the IC ribs. The contact resistances measured as described above are plotted in Figure 9. The three samples with the LSMC CL (full

symbols) have all the same resistance within the uncertainty of the measurement. The samples with the LSCF CL (open symbols) show above 650°C a slight tendency that the resistance increases with the layer thickness, which is given in the legend. At lower temperatures this trend is nearly reverse. Despite the fact that the overall ASR differences are relatively small, especially the ASR cross-over at $\sim 650^{\circ}\text{C}$ seems to be more than "measurement uncertainty" (but a clear uncertainty factor cannot be given). Hence, it seems that the layer thickness does not affect the contact resistance as long as it is below $200\mu\text{m}$. Above this value the thickness may cause and additional ohmic resistance increasing the total contact resistance between IC and cathode. The deviation between LSCF and LSMC here is again explained by the different microstructures, as discussed previously.

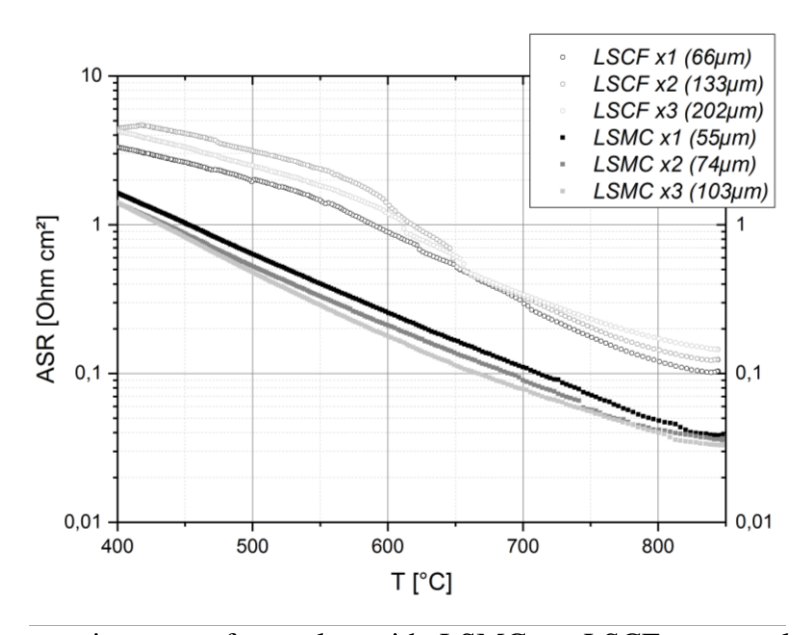


Figure 9. Contact resistances of samples with LSMC or LSCF contact layer of different thicknesses, in dependence on the operation temperature.

CONCLUSIONS

We presented a comparison of various materials for contact layers and protective coatings used in SOC stacks. From the electronic conductivity measurements of LSCF, LCC10, and LSMC we conclude that LSCF is the most applicable material as its conductivity is better than those of LCC10 and LSMC. But this material property is not the only factor to be considered when creating a contact layer. Concerning the microstructure, small particles yield a fine structure that is beneficial for the conduction of electrons. But for a sufficient supply of air to the cathode a coarse structure is required. Thus, we recommend using a coarsely structured, highly porous LSCF contact layer applied by screen printing, which is an easy and quick method.

As the contact layer is also used for leveling height differences during the stack assembly, we recommend keeping the thickness of this layer below 200µm. Above this value the Ohmic contribution to the resistance of the layer increases noticeably.

For the retention of chromium in the interconnector steel, a protective coating of MCF applied by APS offers the best performance due to its dense structure. About this layer it is known that the initial contact resistance as well as the long-term degradation behavior during stack operation is satisfying. The newly developed contact layer applied by WPS and treated with reactive sintering shows a comparable low initial contact resistance. The long-term degradation behavior will soon be tested in a stack experiment.

ACKNOWLEDGEMENTS

The authors thank the BMWI for receiving funding in project No. 03ET6056D. We also thank A.M. and F.H. for provision of material and for discussion...

REFERENCES

- 1. R. Spotorno, P. Piccardo, and G. Schiller, "Effect of Cathode Contacting on Anode Supported Cell Performances," *Journal of The Electrochemical Society,* 163[8] F872-F76 (2016).
- 2. Z. Yang, G. Xia, P. Singh, and J. W. Stevenson, "Electrical contacts between cathodes and metallic interconnects in solid oxide fuel cells," *Journal of Power Sources*, 155[2] 246-52 (2006).
- 3. F. Tietz, H. P. Buchkremer, V. A. C. Haanappel, A. Mai, N. H. Menzler, J. Mertens, W. J. Quadakkers, D. Rutenbeck, S. Uhlenbruck, M. Zahid, and D. Stöver, "Improved Sofc Cathodes and Cathode Contact Layers," pp. 269-74. in 28th International Conference on Advanced Ceramics and Composites A: Ceramic Engineering and Science Proceedings. John Wiley & Sons, Inc., 2008.
- 4. L. Blum, L. G. J. de Haart, J. Malzbender, N. H. Menzler, J. Remmel, and R. Steinberger-Wilckens, "Recent results in Jülich solid oxide fuel cell technology development," *Journal of Power Sources*, 241 477-85 (2013).
- 5. L. Blum, "An Analysis of Contact Problems in Solid Oxide Fuel Cell Stacks Arising from Differences in Thermal Expansion Coefficients," *Electrochimica Acta*, 223 100-08 (2017).
- 6. W. J. Quadakkers, J. Piron Abellan, V. Shemet, and L. Singheiser, "Metallic interconnectors for solid oxide fuel cells a review," *Materials at high temperatures*, 20[2] 115-27 (2003).
- 7. W. J. Quadakkers, J. Pirón-Abellán, and V. Shemet, "Metallic materials in solid oxide fuel cells," *Materials Research*, 7 203-08 (2004).
- 8. P. Huczkowski, N. Christiansen, V. Shemet, L. Niewolak, J. Piron-Abellan, L. Singheiser, and W. J. Quadakkers, "Growth Mechanisms and Electrical Conductivity of Oxide Scales on Ferritic Steels Proposed as Interconnect Materials for SOFC's," *Fuel Cells*, 6[2] 93-99 (2006).
- 9. S. Megel, E. Girdauskaite, V. Sauchuk, M. Kusnezoff, and A. Michaelis, "Area specific resistance of oxide scales grown on ferritic alloys for solid oxide fuel cell interconnects," *Journal of Power Sources*, 196[17] 7136-43 (2011).
- 10. VDM Metals, "Crofer 22 APU Data Sheet No. 4046." in. VDM Metals GmbH, 2010.
- K. Hilpert, D. Das, M. Miller, D. H. Peck, and R. Weiß, "Chromium Vapor Species over Solid Oxide Fuel Cell Interconnect Materials and Their Potential for Degradation Processes," *Journal of The Electrochemical Society*, 143[11] 3642-47 (1996).
- 12. E. Bucher and W. Sitte, "Long-term stability of the oxygen exchange properties of $(\text{La,Sr})1-z(\text{Co,Fe})03-\delta$ in dry and wet atmospheres," *Solid State Ionics*, 192[1] 480-82 (2011).
- 13. N. H. Menzler, D. Sebold, and Q. Fang, "Chromium-Related Degradation of Thin-Film Electrolyte Solid Oxide Fuel Cell Stacks," *Journal of The Electrochemical Society,* 162[12] F1275-F81 (2015).
- 14. N. H. Menzler, D. Sebold, and E. Wessel, "Interaction of La0.58Sr0.40Co0.20Fe0.80O3–δ cathode with volatile Cr in a stack test Scanning electron microscopy and transmission electron microscopy investigations," *Journal of Power Sources*, 254 148-52 (2014).
- 15. A. Beez, X. Yin, N. H. Menzler, R. Spatschek, and M. Bram, "Insight into the Reaction Mechanism of (La0.58Sr0.40)(Co0.20Fe0.80)O3-δ Cathode with Volatile Chromium Species at High Current Density in a Solid Oxide Fuel Cell Stack," *Journal of The Electrochemical Society*, 164[10] F3028-F34 (2017).
- 16. M. V. F. Schlupp, J. W. Kim, A. Brevet, C. Rado, K. Couturier, U. F. Vogt, F. Lefebvre-Joud, and A. Züttel, "Avoiding chromium transport from stainless steel interconnects into contact layers and oxygen electrodes in intermediate temperature solid oxide electrolysis stacks," *Journal of Power Sources*, 270 587-93 (2014).
- 17. B. Talic, H. Falk-Windisch, V. Venkatachalam, P. V. Hendriksen, K. Wiik, and H. L. Lein, "Effect of coating density on oxidation resistance and Cr vaporization from solid oxide fuel cell interconnects," *Journal of Power Sources*, 354 57-67 (2017).
- 18. N. Grünwald, D. Sebold, Y. J. Sohn, N. H. Menzler, and R. Vaßen, "Self-healing atmospheric plasma sprayed Mn1.0Co1.9Fe0.1O4 protective interconnector coatings for solid oxide fuel cells," *Journal of Power Sources*, 363[Supplement C] 185-92 (2017).

- 19. R. Vaßen, N. Grünwald, D. Marcano, N. H. Menzler, R. Mücke, D. Sebold, Y. J. Sohn, and O. Guillon, "Aging of atmospherically plasma sprayed chromium evaporation barriers," *Surface and Coatings Technology*, 291[Supplement C] 115-22 (2016).
- 20. M. Engelbracht, R. Peters, L. Blum, and D. Stolten, "Analysis of a Solid Oxide Fuel Cell System with Low Temperature Anode Off-Gas Recirculation," *Journal of The Electrochemical Society*, 162[9] F982-F87 (2015).
- 21. X. Montero, N. Jordán, J. Pirón-Abellán, F. Tietz, D. Stöver, M. Cassir, and I. Villarreal, "Spinel and Perovskite Protection Layers Between Crofer22APU and La0.8Sr0.2FeO3 Cathode Materials for SOFC Interconnects," *Journal of The Electrochemical Society*, 156[1] B188-B96 (2009).
- 22. X. Montero, F. Tietz, D. Sebold, H. P. Buchkremer, A. Ringuede, M. Cassir, A. Laresgoiti, and I. Villarreal, "MnCo1.9Fe0.1O4 spinel protection layer on commercial ferritic steels for interconnect applications in solid oxide fuel cells," *Journal of Power Sources*, 184[1] 172-79 (2008).
- 23. S. R. Akanda, N. J. Kidner, and M. E. Walter, "Spinel coatings on metallic interconnects: Effect of reduction heat treatment on performance," *Surface & Coatings Technology*, 253 255-60 (2014).
- 24. C. Comminges, M. Zahid, I. Larring, and F. Tietz, "Influence of the Processing Method on the Quality of the Protective Coatings for SOFC Applications," *ECS Transactions*, 25[2] 1403-10 (2009).
- 25. H. Falk-Windisch, J. Claquesin, M. Sattari, J.-E. Svensson, and J. Froitzheim, "Co- and Ce/Co-coated ferritic stainless steel as interconnect material for Intermediate Temperature Solid Oxide Fuel Cells," *Journal of Power Sources*, 343 1-10 (2017).
- 26. J. G. Grolig, J. Froitzheim, and J.-E. Svensson, "Effect of Cerium on the Electrical Properties of a Cobalt Conversion Coating for Solid Oxide Fuel Cell Interconnects A Study Using Impedance Spectroscopy," *Electrochimica Acta*, 184 301-07 (2015).
- 27. M.-F. Han, X. Du, and Z. Liu, "Characterization of La0.8Sr0.2Co0.5Mn0.5O3-δ Coating on Alloy Interconnect in SOFC," *ECS Transactions*, 25[2] 1379-86 (2009).
- 28. J. Hong, M. Bianco, J. Van herle, and R. Steinberger-Wilckens, "Properties of Spinel Protective Coatings Prepared Using Wet Powder Spraying for SOFC Interconnects," *ECS Transactions*, 68[1] 1581-87 (2015).
- 29. S. N. Hosseini, F. Karimzadeh, M. H. Enayati, and N. M. Sammes, "Oxidation and electrical behavior of CuFe2O4 spinel coated Crofer 22 APU stainless steel for SOFC interconnect application," *Solid State Ionics*, 289 95-105 (2016).
- 30. N. J. Magdefrau, L. Chen, E. Y. Sun, J. Yamanis, and M. Aindow, "Formation of spinel reaction layers in manganese cobaltite coated Crofer22 APU for solid oxide fuel cell interconnects," *Journal of Power Sources*, 227 318-26 (2013).
- 31. J. C. W. Mah, A. Muchtar, M. R. Somalu, and M. J. Ghazali, "Metallic interconnects for solid oxide fuel cell: A review on protective coating and deposition techniques," *International Journal of Hydrogen Energy*, 42[14] 9219-29 (2017).
- 32. J. Puranen, J. Lagerbom, L. Hyvärinen, M. Kylmälahti, O. Himanen, M. Pihlatie, J. Kiviaho, and P. Vuoristo, "The Structure and Properties of Plasma Sprayed Iron Oxide Doped Manganese Cobalt Oxide Spinel Coatings for SOFC Metallic Interconnectors," *Journal of Thermal Spray Technology*, 20[1] 154-59 (2011).
- 33. N. Shaigan, W. Qu, D. G. Ivey, and W. X. Chen, "A review of recent progress in coatings, surface modifications and alloy developments for solid oxide fuel cell ferritic stainless steel interconnects," *Journal of Power Sources*, 195[6] 1529-42 (2010).
- 34. J. Tallgren, M. Bianco, J. Mikkola, O. Himanen, M. Rautanen, J. Kiviaho, and J. Van Herle, "Comparison of different manganese-cobalt-iron spinel protective coatings for SOFC interconnects," *12th European SOFC / SOE Forum*, B06[16] 114-24 (2016).
- 35. E. Saoutieff, G. Bertrand, M. Zahid, and L. Gautier, "APS Deposition of MnCo2O4 on Commercial Alloys K41X used as Solid Oxide Fuel Cell Interconnect: The Importance of Post Heat-treatment for Densification of the Protective Layer," *ECS Transactions*, 25[2] 1397-402 (2009).

- 36. Z. G. Yang, G. G. Xia, S. P. Simner, and J. W. Stevenson, "Thermal growth and performance of manganese cobaltite spinel protection layers on ferritic stainless steel SOFC interconnects," *Journal of the Electrochemical Society*, 152[9] A1896-A901 (2005).
- 37. F. Tietz, I. Arul Raj, M. Zahid, and D. Stöver, "Electrical conductivity and thermal expansion of La0.8Sr0.2(Mn,Fe,Co)O3-δ perovskites," *Solid State Ionics*, 177[19–25] 1753-56 (2006).
- 38. F. Tietz, I. A. Raj, M. Zahid, A. Mai, and D. Stöver, "Survey of the quasi-ternary system La0.8Sr0.2MnO3–La0.8Sr0.2CoO3–La0.8Sr0.2FeO3," *Progress in Solid State Chemistry*, 35[2] 539-43 (2007).
- 39. D. Lee, Y.-L. Lee, W. T. Hong, M. D. Biegalski, D. Morgan, and Y. Shao-Horn, "Oxygen surface exchange kinetics and stability of (La,Sr)2CoO4+/-[small delta]/La1-xSrxMO3-[small delta] (M = Co and Fe) hetero-interfaces at intermediate temperatures," *Journal of Materials Chemistry A*, 3[5] 2144-57 (2015).
- 40. J. N. Davis, K. F. Ludwig, K. E. Smith, J. C. Woicik, S. Gopalan, U. B. Pal, and S. N. Basu, "Surface Segregation in Lanthanum Strontium Manganite Thin Films and Its Potential Effect on the Oxygen Reduction Reaction," *Journal of The Electrochemical Society*, 164[10] F3091-F96 (2017).
- 41. J. Hardy, J. Stevenson, P. Singh, M. Mahapatra, E. Wachsman, M. Liu, and K. Gerdes, "Effects of Humidity on Solid Oxide Fuel Cell Cathodes." in. Edited by U. S. D. o. Energy. Pacific Northwest National Laboratory, Battelle, 2015.
- 42. E. Bucher, W. Sitte, F. Klauser, and E. Bertel, "Oxygen exchange kinetics of La0.58Sr0.4Co0.2Fe0.8O3 at 600°C in dry and humid atmospheres," *Solid State Ionics*, 191[1] 61-67 (2011).
- 43. D. Rembelski, J. P. Viricelle, L. Combemale, and M. Rieu, "Characterization and Comparison of Different Cathode Materials for SC-SOFC: LSM, BSCF, SSC, and LSCF," *Fuel Cells*, 12[2] 256-64 (2012).
- 44. M. C. Tucker, L. Cheng, and L. C. DeJonghe, "Selection of cathode contact materials for solid oxide fuel cells," *Journal of Power Sources*, 196[20] 8313-22 (2011).
- 45. J. H. Zhu and H. Ghezel-Ayagh, "Cathode-side electrical contact and contact materials for solid oxide fuel cell stacking: A review," *International Journal of Hydrogen Energy*, 42[38] 24278-300 (2017).
- 46. F. Tietz, A. Schmidt, and M. Zahid, "Investigation of the quasi-ternary system LaMnO3-LaCoO3-"LaCuO3"-I: the series La(Mn0.5Co0.5)(1-x)CuxO3-delta," *Journal of Solid State Chemistry*, 177[3] 745-51 (2004).
- 47. F. Tietz, I. A. Raj, Q. X. Fu, and M. Zahid, "Investigation of the quasi-ternary system LaMnO3-LaCoO3-"LaCuO3". II: The series LaMn0.25-x Co0.75-x Cu-2x O3-delta and LaMn0.75-x Co0.25-x Cu-2x O3-delta," *Journal of Materials Science*, 44[18] 4883-91 (2009).
- 48. N. H. Menzler and V. A. C. Haanappel, "Influence of anode thickness on the power output of solid oxide fuel cells with (La,Sr)(Co,Fe)-type cathode," *Journal of Power Sources*, 195[16] 5340-43 (2010).
- 49. A. Petric and H. Ling, "Electrical Conductivity and Thermal Expansion of Spinels at Elevated Temperatures," *Journal of the American Ceramic Society*, 90[5] 1515-20 (2007).
- 50. L. Blum, Q. Fang, L. De Haart, J. Malzbender, N. Margaritis, N. Menzler, and R. Peters, "SOC development at Forschungszentrum Jülich," *ECS Transactions*, 78[1] 1791-804 (2017).
- 51. J. Mizusaki, S. Tsuchiya, K. Waragai, H. Tagawa, Y. Arai, and Y. Kuwayama, "Simple mathematical model for the electrical conductivity of highly porous ceramics," *Journal of the American Ceramic Society*, 79[1] 109-13 (1996).
- 52. Z. G. Yang, G. G. Xia, X. H. Li, and J. W. Stevenson, "(Mn,Co)(3)O(4) spinel coatings on ferritic stainless steels for SOFC interconnect applications," *International Journal of Hydrogen Energy*, 32[16] 3648-54 (2007).
- 53. J.-E. Hong, A. Masi, M. Bianco, J. Van Herle, and R. Steinberger-Wilckens, "Insight of Reactive Sintering in Manganese Cobalt Spinel Oxide of Protective Layer for Solid Oxide Fuel Cell Metallic Interconnects," *12th European SOFC / SOE Forum,* B06[21] 133-36 (2016).